# $CO_2$ Network for Thermal Management in Buildings


## Abstract

This study presents a novel concept to provide space heating and cooling inside buildings using a thermal distribution network. The thermal network consists of a single-pipe loop circulating two-phase $CO_2$ as the heat carrier fluid and connects all the thermal zones together. It offers simultaneous heating and cooling in buildings as well as heat recovery between the zones.

The proposed system with all its associated components were modelled using MATLAB and hypothetically applied in small office buildings in three cities with known yearly load profiles. Consequently, the annual performance of the thermal network was evaluated for those offices and showcased the high potential of this novel system for buildings with simultaneous heating and cooling demand in mild climate regions.


## Introduction

The building sector is a significant contributor to the total energy use in Canada, particularly due to space heating and cooling, and it is thus associated with greenhouse gas (GHG) emissions and other environmental issues. Addressing energy use in buildings calls for a broader effort to promote the integration of renewable energy sources and energy-efficient heating and cooling systems. One strategy is applying low-exergy systems characterized by having small temperature differences for heating and cooling (Torio & Schmidt, 2011). Decentralized heating and cooling is a practical low-exergy system consisting of a low-grade energy source distribution system. In other words, the distribution system is a loop that supplies a low-temperature heating/high-temperature cooling source, and local heat pumps (HPs) are connected to this loop to address heating and cooling demands in a building efficiently. The local HP provides the flexibility to have an individual unit at each zone to match supply and demand effectively.

The only system currently incorporating decentralized energy transformation in building scale is the so-called water loop heat pump (WLHP) system. WLHP systems incorporate a water loop as a hydronic heating/cooling system. The circulated water simultaneously provides heating and cooling for different thermal zones through HPs. Eventually, selected cooling/heating systems (e.g., cooling towers and boilers) maintain the temperature of the loop within a certain range. At present, the researches on the WLHP have concentrated on analyzing its energy-saving rate and applications. Mast and Leibundgut (2012) concluded that HPs connected to the water-loop require a certain minimum Carnot efficiency to provide a competitive performance than conventional systems. Lian et al. (2005) suggested the application of WLHP based on the ratio of the core-zone load over the perimeter-zone load. According to their results, cooling-dominant buildings are not a good candidate for WLHP systems. Yu (2017) highlighted that buildings with simultaneous heating and cooling loads are the best candidates for decentralized systems. They also pointed out that improving the efficiency of the local units and the design of the hydronic loop in terms of its temperature and its hydrodynamics are important new subjects for related researches.

Circulating water in a temperature ranging between 16°C and 32°C (McQuay Inc., 1999) still allows significant heat losses from the distribution system in a WLHP. In addition, the varying temperature of the loop harms the performance of connected HPs by increasing the temperature lift. In order to efficiently address the total demand, a sufficiently high water mass flow rate is required. Moreover, there is a concern regarding the issues related to the water leakage from the loop.

A similar decentralized thermal energy transformation concept has been applied in urban areas using the district generation and cogeneration systems. Whereas 2$^{nd}$ and 3$^{rd}$ generation district heating systems used water as the heat carrier fluid, circulating a refrigerant expanded the application of the system for cold distribution and suggested an alternative method to take advantage of the latent heat (Werner, 2017). Weber and Favrat (2010) proposed employing two-phase $CO_2$ as the refrigerant in a district energy network (for both heating and cooling). In their proposal, the district network consists of a two-pipe circuit distributing saturated liquid and gas $CO_2$ in a temperature range between 12°C and 18°C. Local heat pumps connected to the network provide the heating and cooling energy required for air conditioning, hot water, and refrigeration in buildings in the district. According to their calculation, comparing $CO_2$ as an alternative for water network, the piping size and the yearly pumping energy may reduce by 58% and 38%, respectively. Henchoz et al. (2017) built an experimental setup to mimic the $CO_2$ distribution energy system, and no major issues were reported concerning the relatively high-pressure operation of $CO_2$.

Although $CO_2$ district energy systems incorporate the concept of decentralized energy transformation, the two-pipe arrangement (one vapor, one liquid) cannot be efficiently applied in buildings in which their thermal load profile varies more frequently. The dynamic behavior of buildings, where systems frequently switch between cooling and heating during the shoulder seasons, cannot be addressed appropriately. Exploring the potentials of saturated $CO_2$ as a heat carrier fluid offers a new alternative to improve the current air conditioning system in buildings. Lower operational temperature (as low as the room temperature), the insignificant heat loss of the distribution pipes, and lower pumping energy consumption guide this research to a new decentralized energy transformation system for buildings.

In this article, the novel concept of a single-pipe two phase $CO_2$ network for building applications is explained. Then the model developed to simulate the performance of the system is explained. By employing the model, the potentials of the system to effectively provide heating and cooling in buildings are explored through its hypothetical application in a small office building.

# Methodology

## Description of the $CO_2$ Thermal Network System

This section describes a novel technology to manage thermal energy inside buildings. It facilitates heat recovery, space conditioning, and hot water production in newly constructed or retrofitted buildings. The proposed innovative thermal energy network is a single-pipe. It is spread in the entire building circulating two-phase $CO_2$; hence all thermal zones can be connected to this pipe via a local HP. The main loop operates at a constant temperature close to the room condition. This strategy minimizes heat losses, and the piping system does not need any insulation. Depending on the thermal load, each HP produces either cooling or heating and rejects or extracts heat from the main loop, respectively. Indeed, $CO_2$ continuously condenses or evaporates along the main loop. Meanwhile, a variable speed compressor as the circulation mechanism keeps the state of the refrigerant unchanged at the end of each cycle by altering its flowrate.

Circulating two-phase $CO_2$ makes use of the latent heat instead of the less concentrated sensible heat. Consequently, smaller pipe dimensions and distribution systems are required compared to the conventional spacious and bulky air ducting or a water loop. As all the HPs are connected to the same fluid stream, the rejected heat from one unit can be used in another, using full heat recovery potential in a building. All thermal zones exchange heat with each other regardless of their physical distance in a building. Meanwhile, to compensate for the network's deficient/excess energy content, local renewable energy sources (e.g., geothermal heat exchangers, solar thermal collectors, and/or air coolers) are connected to the same loop. It employs compressors as the circulation mechanism, facilitating integrating different grade thermal energy sources, without consuming additional energy to balance the network. $CO_2$ is compressed to an appropriate pressure to exchange heat freely with a cooling source, expanded to the saturated pressure equivalent to the operating temperature (17-23°C), and circulated as a two-phase flow in the entire building. Finally, if there is a deficit of energy, it is expanded to an appropriate pressure to be heated freely by an external source. Depending on the thermal loads, the system may operate either in two or three pressure levels: discharge pressure (high pressure), intermediate pressure (two-phase line), and suction pressure (low pressure). The high and low pressures are set corresponding to the connected renewable source to balance the excess or deficit of energy in the network. Figure 1 presents a schematic application of the $CO_2$ thermal network in a building with the possibility of having air/ground and solar sources of energy to balance the network.

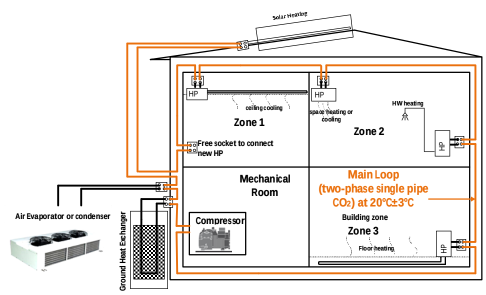


*Figure 1 Schematic of a $CO_2$ Network in a building*

## Model Description

A numerical model is developed with the MATLAB programming software (Matlab, 2019) to simulate the performance of the $CO_2$ network for buildings with multiple thermal zones. The model is a quasi-steady-state model, which receives hourly load profiles of thermal zones and weather conditions. The main components are a variable speed compressor, three heat exchangers, three expansion valves, one receiver, two auxiliary heater and cooler, and all the connected HPs. Figure 2 presents the process flow diagram (PFD) of the system with *n* connected HPs. The modeling of each component is discussed separately in this section. The model provides enthalpy and pressure state of $CO_2$ all around the system (black nodes in Figure 2) at each simulation time step.

<u>Compressor:</u>

The compressor sub-model is developed to calculate the $CO_2$ mass flowrate and work of the compressor. A variable-speed compressor is considered. Both volumetric and isentropic efficiencies are calculated as a function of pressure ratio (Figure 2, the pressure at point 1 over the pressure at point 12+n) at the speed of 60 Hz at which the compressor has the maximum mechanical efficiency. These functions are set as the reference efficiencies and derived with the consultation of manufacturer data of a $CO_2$ compressor as follow:

$$\eta_{60} = f\left({}^{P_{dis-comp}}/_{P_{suc-comp}}\right) \tag{1}$$

For other speeds, the ratio of the efficiencies to the reference is calculated using the frequency ratio as follow:

$$^{\eta}/_{\eta_{60}} = f(f_r) \tag{2}$$

Here, $\eta$ is the efficiencies, $\eta_{60}$ is the efficiency at 60 Hz, $P_{dis\text{-}comp}$ is the pressure at the discharge of the compressor, $P_{suc\text{-}comp}$ is the pressure at the suction of the compressor, and $f_r$ is the compressor frequency ratio ($f/f_{60}$). The relation to the speed of the compressor is also derived from the manufacture datasheet. It is assumed that the speed varies between 0 to 70 Hz. The work of the compressor is calculated using isentropic efficiency as follow:

$$W_{comp.} = \frac{H_{dis-com,isen} - H_{suc-comp}}{\eta_{isen}} \tag{3}$$

where $H_{dis\text{-}comp,isen}$ is the isentropic enthalpy at the discharge of the compressor, $H_{suc\text{-}comp}$ is the enthalpy at the suction of the compressor, and $\eta_{isen}$ is the calculated isentropic efficiency at the operating speed and pressure ratio. Eventually, the enthalpy at the discharge of the compressor and the $CO_2$ mass flowrate are calculated as:

$$H_{dis-comp} = H_{suc-comp} + W_{comp} \tag{4}$$

$$\dot{M} = \rho_{suc-comp} * \eta_{vol} * V_{comp} * f_r \tag{5}$$

Here, $\rho_{suc\text{-}comp}$ is the density at the suction of the compressor, $V_{comp}$ is the swept volume rate at 60 Hz, and $\eta_{vol}$ is the volumetric efficiency at the operating speed and pressure ratio.

Heat exchangers (HXs):

The model is equipped with two air-$CO_2$ HXs to rebalance the network by heating/cooling $CO_2$ when it is required. The cooler is a gas cooler (GC) with single-phase $CO_2$ on one side and outdoor air on the other side. The heater works as an evaporator that exchanges heat between outdoor air and two-phase $CO_2$. In addition, the model is equipped with an internal heat exchanger (IHX), which provides the required superheat in the suction of the compressor. Single phase $CO_2$ flows on both sides of this HX. All the HXs are modeled using the ε-NTU method:

$$NTU = \frac{UA}{C_{min}} \tag{6}$$

$$C_{min} = min[C_p * \dot{m}] \tag{7}$$

where $NTU$ is the number of transfer units, $UA$ is the overall heat transfer coefficient, $C_p$ is the specific isobaric heat capacity, $\dot{m}$ is the mass flowrate, and $C_{min}$ is the minimum value of $(C_p * \dot{m})$ between the fluids on both sides of a HX. For the GC and IHX, the range of calculated $NTU$ and the type of HX are used to determine its efficiency ($\varepsilon$). For the evaporator, $\varepsilon$ is calculated as follow:

$$\varepsilon = 1 - e^{(-NTU)} \tag{8}$$

The heat transfer rate at each HX is given by:

$$q_{HX} = \varepsilon * C_{min} * (T_{in,H} - T_{in,C}) \tag{9}$$

where $T_{in,H}$ and $T_{in,C}$ are the inlet temperature on the hot-side and the cold-side of a HX, respectively. It is assumed that the HXs are perfectly insulated, and there is no heat loss.

During simulation periods when the outdoor air does not have enough quality to cool or heat $CO_2$, the excess or deficit of energy in the network is rebalanced using an auxiliary cooler or heater, respectively. A boiler with 90% efficiency is considered as the auxiliary heater, while a chiller with the coefficient of performance (COP) equal to 1 is assigned as the auxiliary cooler.

Expansion Valve (EV) and Receiver:

The model is equipped with three EVs, which adjust the operating pressure of the network. EV1 controls the discharge pressure of the compressor based on the operation mode of the system. When the networks operate in cooling demand, EV1 sets the discharge pressure accordingly to have free cooling in HX1 using outdoor air. $CO_2$ expands to the set-point operating pressure in the mainline inside a building. The mainline pressure always follows the receiver's pressure controlled by EV2 (flash-gas valve). EV2 actuates to keep the receiver at its set-point pressure, equivalent to the required $CO_2$ saturated temperature in the mainline. EV3 expands saturated liquid from the receiver to an appropriate pressure to evaporate $CO_2$ in HX2 and satisfy a constant superheat temperature at the suction of the compressor. All the EVs are assumed to be isenthalpic in this model.

The receiver is also modeled at a constant pressure set by EV2.

Building and its HPs:

The simulated building is represented with its thermal zones and their corresponding hourly load profiles. The thermal energy balance of each zone is calculated hourly, taking into account the load and the heat transfer from/to the mainline through the connected HPs.

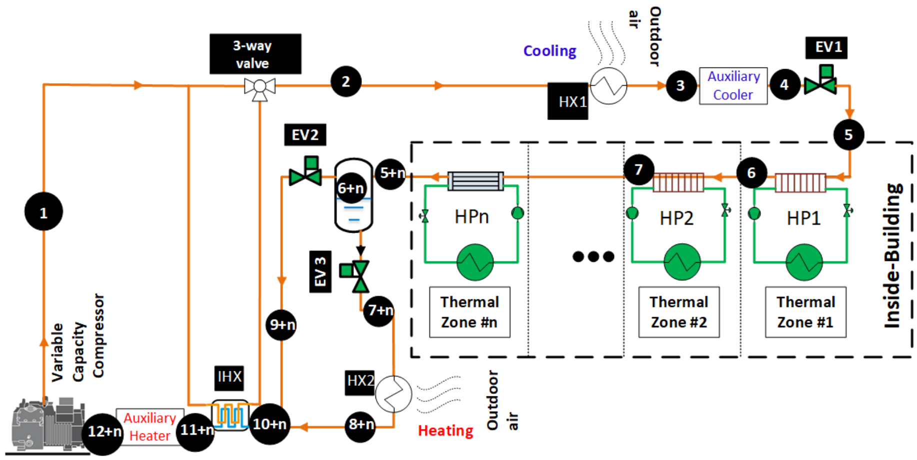


*Figure 2 PDF and components of the model*

$$Th - ENE_i^j = Th - ENE_i^{j-1} + (Load_i^j + Q_{HP,i}^j) * \Delta t \quad (10)$$

where *Th-ENE*, *Load* and $Q_{HP}$ are the thermal energy balance, thermal load and heat transfer rate of the HP at the $i^{th}$ zone, respectively. *j* represents the discretized simulation time with *Δt* simulation time-step (it is set to 1h in this study). The balance at each simulation time step decides the operating mode of the corresponding HP.

The connected HP at each zone is treated as a low lift temperature heat pump (LLTHP) with high efficiency. Those HPs utilize the mainline as their source/sink of energy while operating to keep each zone at a temperature in the comfort range (20°C to 24°C). Therefore, the assumption of LLTHP is very realistic. These HPs operate with COP between 10 to 17 (Gasser et al., 2017). In the current study, HPs were simulated as a unit to provide heating and cooling with COP=10.

<u>Modeling approach:</u>

The network may operate in two modes depending on the demands of the connected zones: heating dominant and cooling dominant. In the heating dominant mode, HPs working in heating modes outnumber those working on cooling mode, while the reverse situation is called cooling dominant mode. The model is programmed with two separate algorithms regarding the operating mode of the system. Figure 3 presents the logic flow chart of the developed model at each time step.

At the end of each time step, the model provides the thermal energy balance of each connected zone, total energy consumption (EC) of the system, and the COP of the network to provide heating and cooling in the building. The total EC includes the work of the compressor and the connected HPs. In addition, the auxiliary heater and cooler may need to operate on occasions when the outdoor air does not have sufficient thermal quality to reject/supply the excess/deficit of energy in the network. On those occasions, auxiliaries contribute to the total EC of the system. Therefore, the total EC at each simulation time step is calculated:

$$EC_{tot}^j = EC_{comp}^j + \sum_{i=1}^{n} EC_{HP,i}^j + EC_{Aux}^j \quad (11)$$

where $EC^j_{comp}$, $EC^j_{HP,i}$ and $EC^j_{Aux}$ are the compressor, the associated HP to zone *i*, and the auxiliary EC at time *j*, respectively. The COP of the network is given as:

$$COP^j = \frac{\sum_{i=1}^{n} abs[Q_{HP,i}^j]}{EC_{tot}^j} \quad (12)$$

Here, the numerator gives the total thermal energy provided by the network to the building via HPs. Year-round cumulative performance of the network is quantified as:

$$COP_{cumulative} = \frac{\sum_{j=0\,[h]}^{8760\,[h]} \sum_{i=1}^{n} abs[Q_{HP,i}^j]}{\sum_{j=0\,[h]}^{8760\,[h]} EC_{tot}^j} \quad (13)$$

**Case study description**

As case studies, the network was deployed hypothetically in small office buildings in Canada. Tamasauskas et al. (Tamasauskas, Kegel, & Blake, 2018) provided the load profiles representing such office buildings. These buildings' heating and cooling loads were obtained using a set of region-specific small office models developed in EnergyPLUS. Table 1 provides parameters characterizing the simulated office.

*Table 1: Parameters characterizing a small office*

| Parameter | Value |
|---|---|
| Total Floors | 1 |
| Total Floor Area | 511 $m^2$ |
| Aspect Ratio | 1.50 |
| Glazing Percent | 21% |

The occupied area of the office is divided into five separate thermal zones: four perimeters and one core zone. They are named based on their orientations. Figure 4 schematically depicts the hypothetical deployment of a $CO_2$ network in this office building. It needs to be highlighted that the figure is not to scale. Moreover, heating and cooling demands of each thermal zone are characterized based on their peak, total demand, and duration in a year. One can consult Table 3 in the Appendix section to study those specific details.

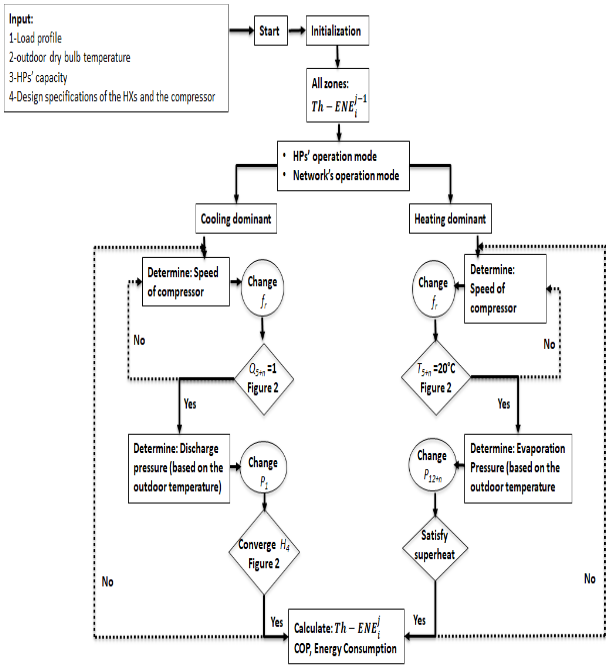


*Figure 3 Logic flow chart to model $CO_2$ network*

While outdoor air is utilized as the integrated renewable source of energy, three regions are selected in this study to demonstrate the impact of different climates. Table 2 summarizes these climatic parameters. For the simulation, the appropriate CWEC weather file at a time step of 1 hr is linked with the developed code in MATLAB.

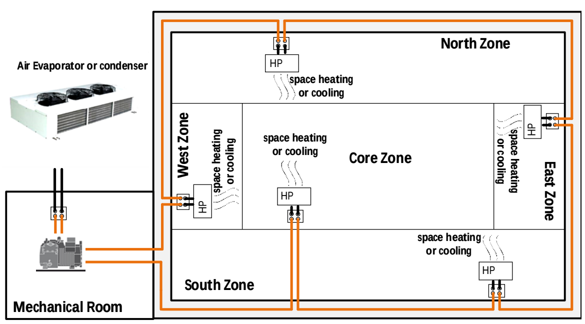


*Figure 4: Hypothetical deployment of $CO_2$ network in a small office building with five thermal zones*

*Table 2: Climate parameters summary ((CCBFC, 2010) and (CCBFC, 2011))*

| | Montreal (QC) | Vancouver (BC) | Whitehorse (Yu) |
|---|---|---|---|
| **NECB [1]CZ** | Zone 6 | Zone 4 | Zone 7B |
| **HDD(18°C)** | 4200 | 2950 | 6850 |
| **Heat [2]$T_D$** | -23 | -7 | -41 |
| **Cool [3]$T_D$** | 30/23 | 28/20 | 25/15 |

[1]CZ: Climate zone, [2]Dry bulb design temperature [°C], [3]Dry bulb/Wet bulb design temperature [°C]

## Results and Discussion

$CO_2$ network performance was simulated annually for all the three cities, and the evolution of their $COP_{cumulative}$ is presented in Figure 5-a. Herein, the x-axis shows the time of a year in hour starting January 1st. The highest performance is obtained for the office located in Vancouver, which has a milder climate than the other cities. Its annual $COP_{cumulative}$ is equal to 3.85, 20% and 25% higher than the offices located in Montreal and Whitehorse, respectively.

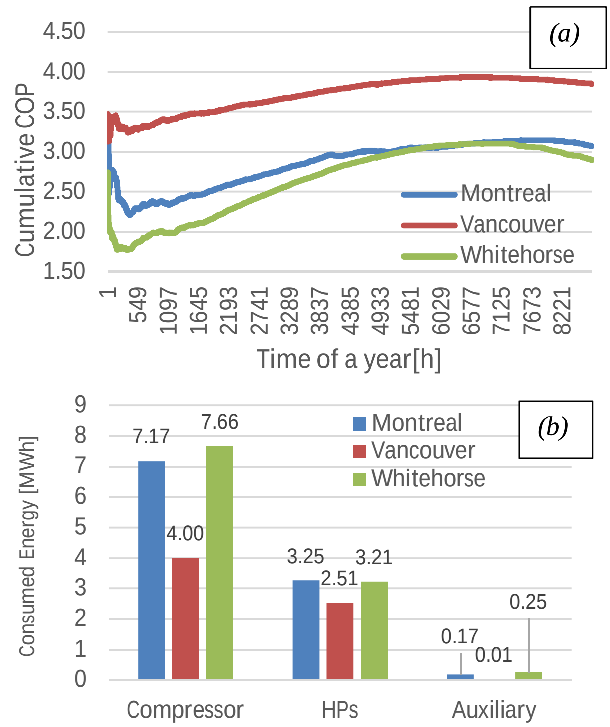


*Figure 5: a) Year round evolution of $COP_{cumulative}$ b) Contributors' share in year-round total EC*

Investigating all the three profiles highlights the similarity in their trend. All start with overall negative derivatives in winter. Later it rises at the end of winter and during spring, when the weather gets milder and the chance of having simultaneous heating and cooling demands increases. When buildings have both heating and cooling loads, removed energy from one zone can be recovered and utilized by the network to condition another zone fully or partially. Moreover, exchanging energy inside a building through the mainline reduces the required energy consumption to rebalance the network using external sources. In addition to more frequent simultaneous heating and cooling, the milder outdoor temperature has a higher quality to rebalance the network with no need for the auxiliaries to operate. In contrast, during the summer, the derivative reduces in all the profiles due to the warmer weather condition. Higher outdoor temperature causes a cooling-only load in all the zones frequently, and there would be less opportunity for heat recovery inside the buildings. In addition, outdoor air has a lower quality to cool down the network; hence the auxiliary cooler would operate often.

As the network is equipped with appropriately sized components, the weather condition is the only parameter that imposes the need for auxiliaries. Such an impact can be realized in the studied cities. In fact, Vancouver had the smallest share of auxiliary in its annual energy consumption due to its milder weather condition. The contribution of the compressor, HPs, and auxiliaries in the annual EC are presented and compared in Figure 5-b for all the simulated offices.

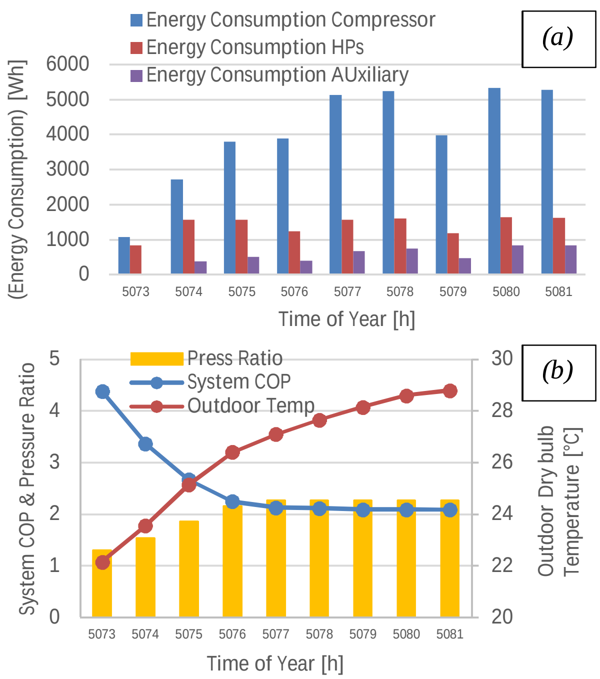


*Figure 6: $CO_2$ network performance in the warmest time of a year (the office in Montreal)*

Focusing on the contribution of HPs and compressors, one can notice that the office in Montreal has a larger share of HPs and a lower share of the compressor than the one in Whitehorse. It implies that the HPs work longer in Montreal, and the building's thermal demand is higher. However, the compressor operates with a lower average pressure ratio and speeds due to the milder outdoor temperature and more frequent simultaneous heating and cooling demand in the office in Montreal. Therefore, the compressor's share of EC is lower.

In order to investigate the performance of the $CO_2$ network system in detail, this study focuses on the operation of the system during the warmest and coldest time of the year in Montreal. Figure 6-a delivers the system's EC during the warmest time of a year in which the outdoor temperature rises as high as 29°C in July. Meanwhile, Figure 6-b presents system COP, compressor's pressure ratio, and the outdoor dry bulb temperature at the same period. One can notice that after a certain temperature, the outdoor air does not have sufficient quality to cool down the network, and the auxiliary cooler is employed to rebalance the network. Moreover, the compressor's EC increases due to its higher pressure ratio, as presented in Figure 6-b. On some occasions (e.g., at 5079 h), the lower compressor's EC is caused by lower speed due to fewer active HPs inside the office at those specific time. The system COP thus drops as the outdoor temperature increases. The system performs within a COP ranges from 4.5 to 2 in that period, which has a high competence comparing to the current technologies[1]. COP values show a high dependence on the performance of the HPs and the size of the system.

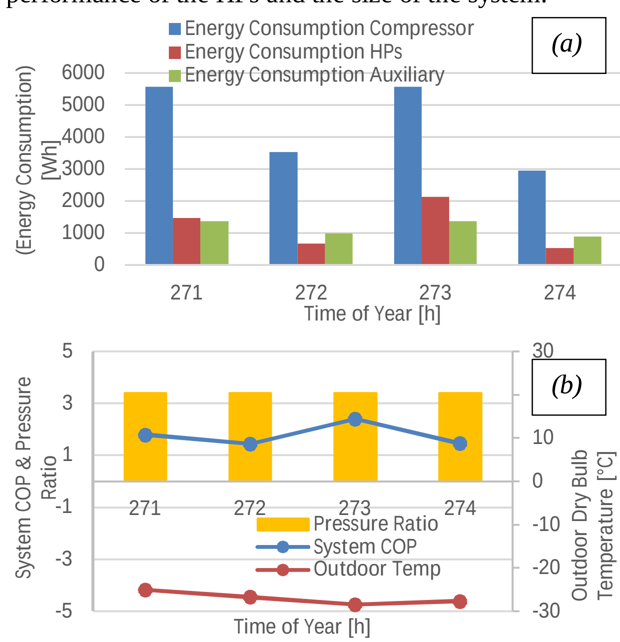


*Figure 7: $CO_2$ network performance in the coldest time of a year (the office in Montreal)*

The coldest time of a year was investigated for the office located in Montreal. During this period, the outdoor temperature drops to -30°C, and the air does not have enough quality to heat the network. Despite the compressor operating with its highest pressure ratio, the auxiliary heater needs to work continuously to rebalance the $CO_2$ network, as presented in Figure 7. Like the summer, the compressor's EC increases due to its higher pressure ratio, as presented in Figure 7-b. Meanwhile, on some occasions (e.g., at 272 h), the lower compressor's EC is caused by lower speed due to fewer active HPs

[1] To compare with other technologies in the same office building, one may consult (Tamasauskas et al., 2018)

inside the office at those specific time. The network operates with a promising performance during the coldest time of a year as the calculated COP is around 2. Again, COP values are subject to the performance of internal HPs and the size of a system. Performance can be improved by employing more efficient indoor units.

The highest potential for $CO_2$ network systems is in buildings with longer simultaneous heating and cooling demands. The vocation of a building (office buildings, sports complexes, etc.) and climate are the influential parameters that create both demands in a building at the same time. In offices, the occasions with both heating and cooling demand occur more often in shoulder seasons. Thus, the performance of the system is investigated on a couple of occasions with both heating and cooling demands in the office in Montreal during April. Figure 8 showcases: a) system COP and b) the breakdown of its EC in five occasions with mixed loads. The highlights of these occasions are the significantly lower compressor EC and higher system COP. The moderate weather condition and lower required $CO_2$ mass flowrate in the network reduce the work of the compressor to circulate $CO_2$ in the network. In addition, the auxiliaries are not called upon in the shoulder seasons with milder outdoor temperatures. Moreover, higher rates of heat recovery between the zones push system COP up to 6. The higher recovery is perceived by evaluating the value of network load (yellow bar) in Figure 8-b. It quantifies the amount of thermal energy that needs to be either rejected or injected into the system to be rebalanced. Its lower value implies a higher recovery between the connected zones.

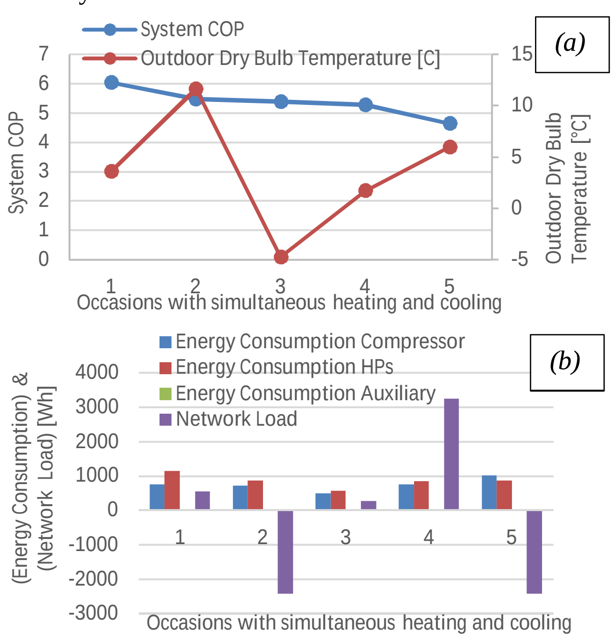


*Figure 8: $CO_2$ performance in a shoulder season (the office in Montreal)*

Consequently, the highest potential to employ a $CO_2$ network would be for buildings located in moderate climates and come with more frequent heating and cooling demand throughout the year.

## Conclusion

This paper has introduced a novel technology for thermal management in buildings. It proposes a single-pipe thermal network, which connects to all thermal zones in a building to provide heating, cooling, and heat recovery inside that built environment. Two-phase $CO_2$ is employed as the heat carrier fluid. Variable speed compressors circulate $CO_2$ and adjust the operating pressures to maximize system performance. A detailed model was developed using MATLAB programming software and deployed hypothetically in a small office building. To analyze different climate zones, the load profiles of the same office in three regions in Canada were utilized.

It has been observed that the system has higher potential in buildings located in moderate climate regions. In those regions, both heating and cooling are simultaneously demanded in a more extended portion of a year. On those occasions, the $CO_2$ network can efficiently recover thermal energy between the zones and reduce the total EC for space heating and cooling. Apart from the effect of climate, building function would specify the types of demand in the thermal zones. Generally, buildings characterized by simultaneous heating and cooling demand (e.g., office buildings and data centers) would be the best candidates equipped with a $CO_2$ thermal network system.

The future work will consider the cost analysis of the proposed system based on the initial and operating costs. This will provide a better understanding of the potential saving of the system, in addition to its simplicity and flexibility.

## Acknowledgment


The authors would like to acknowledge the funding received by the Office of Energy Research and Development (OERD) of Canada through the ecoENERGY Innovation Initiative and Energy Innovation Program to support this research.


## Reference


(CCBFC), C. C. on B. and F. C. (2010). *National Building Code of Canada 2010 Volume 2*. Ottawa: National Research Council of Canada.

(CCBFC), C. C. on B. and F. C. (2011). *National Energy Code of Canada for Buildings (NECB)*. Ottawa: National Research Council of Canada.

Gasser, L., Flück, S., Kleingries, M., Meier, C., Bätschmann, M., & Wellig, B. (2017). High efficiency heat pumps for low temperature lift applications. *12th IEA Heat Pump Conference*, 11.

Henchoz, S., Favrat, D., Marechal, F., & Girardin, L. (2017). Novel district heating and cooling energy network using CO 2 as a heat and mass transfer fluid. *12th IEA Heat Pump Conference 2017*, *36*(1), 1–11.

Lian, Z., Park, S. R., Huang, W., Baik, Y. J., & Yao, Y. (2005). Conception of combination of gas-engine-driven heat pump and water-loop heat pump system. *International Journal of Refrigeration*, *28*(6), 810–819. https://doi.org/10.1016/j.ijrefrig.2005.02.004

Mast, M., & Leibundgut, H. (2012). Introduction and analysis of a concept for decentralized heat pumping in hydronic networks. *Energy and Buildings*, *54*, 461–469. https://doi.org/10.1016/j.enbuild.2012.06.021

Matlab. (2019). Matlab version 9.7.0 (R2019b). Natick, Massachusetts: The MathWorks Inc.

McQuay Inc. (1999). *Water-source heat pump design manual*.

Tamasauskas, J., Kegel, M., & Blake, J. (2018). The Potential of Heat Pump Technologies for the Replacement of Rooftop Units in Small Commercial Buildings Conventional Air-Source Heat Pump. *Proceedings of ESIM 2018, the 10th Conference of IBPSA-Canada, Montreal, Quebec, Canada, May 9-10, 2018*, 212–221.

Torio, H., & Schmidt, D. (2011). *Exergy Assessment Guidebook for the Built Environment-Annex 49 Summary report*. Stuttgart.

Weber, C., & Favrat, D. (2010). Conventional and advanced CO2 based district energy systems. *Energy*, *35*(12), 5070–5081. https://doi.org/10.1016/j.energy.2010.08.008

Werner, S. (2017). International review of district heating and cooling. *Energy*, 1–15. https://doi.org/10.1016/j.energy.2017.04.045

Yu, Q. D. (2017). Theory of energy level and its application in water-loop heat pump system. *Applied Thermal Engineering*, *119*, 269–274. https://doi.org/10.1016/j.applthermaleng.2017.03.068

# Appendix

Table 3 characterizes the load profile of those office buildings in all the three studied cities.

*Table 3: Load characterization in the simulated buildings*

| | Zone | West | | East | | North | | South | | Core | |
|---|---|---|---|---|---|---|---|---|---|---|---|
| | | Heating | Cooling | Heating | Cooling | Heating | Cooling | Heating | Cooling | Heating | Cooling |
| Montreal | Total Demand [kWh] | 1944 | 3124 | 1749 | 3090 | 2833 | 4236 | 2085 | 5714 | 928 | 6903 |
| | Peak Load [kW] | 3.32 | 4.41 | 3.31 | 3.98 | 5.28 | 3.69 | 5.14 | 4.67 | 4.26 | 4.10 |
| | Ratio Total Demand to Core | 2.09 | 0.45 | 1.88 | 0.45 | 3.05 | 0.61 | 2.25 | 0.83 | 1.00 | 1.00 |
| | Ratio Max. Load to Core zone | 0.78 | 1.08 | 0.78 | 0.97 | 1.24 | 0.90 | 1.21 | 1.14 | 1.00 | 1.00 |
| | Total Demand Duration [h] | 5108 | 3652 | 4602 | 4158 | 3545 | 5215 | 3049 | 5711 | 1700 | 7060 |
| | Ratio Total Duration to Core | 3.00 | 0.52 | 2.71 | 0.59 | 2.09 | 0.74 | 1.79 | 0.81 | 1.00 | 1.00 |
| Vancouver | Total Demand [kWh] | 924 | 2714 | 806 | 2581 | 1113 | 4267 | 920 | 4341 | 395 | 7092 |
| | Peak Load [kW] | 2.45 | 4.15 | 2.45 | 3.78 | 3.84 | 3.18 | 3.49 | 5.42 | 3.46 | 3.72 |
| | Ratio Total Demand to Core | 2.34 | 0.38 | 2.04 | 0.36 | 2.82 | 0.60 | 2.33 | 0.61 | 1.00 | 1.00 |
| | Ratio Max. Load to Core zone | 0.71 | 1.12 | 0.71 | 1.02 | 1.11 | 0.85 | 1.01 | 1.46 | 1.00 | 1.00 |
| | Total Demand Duration [h] | 4818 | 3942 | 3918 | 4842 | 2023 | 6737 | 1599 | 3429 | 796 | 7964 |
| | Ratio Total Duration to Core | 6.05 | 0.49 | 4.92 | 0.61 | 2.54 | 0.85 | 2.01 | 0.43 | 1.00 | 1.00 |
| Whitehorse | Total Demand [kWh] | 2892 | 1946 | 2796 | 2080 | 4384 | 3130 | 3812 | 3562 | 1525 | 5994 |
| | Peak Load [kW] | 3.98 | 4.19 | 3.97 | 3.97 | 6.21 | 3.25 | 6.25 | 5.66 | 5.08 | 3.67 |
| | Ratio Total Demand to Core | 1.90 | 0.32 | 1.83 | 0.35 | 2.87 | 0.52 | 2.50 | 0.59 | 1.00 | 1.00 |
| | Ratio Max. Load to Core zone | 0.78 | 1.14 | 0.78 | 1.08 | 1.22 | 0.88 | 1.23 | 1.54 | 1.00 | 1.00 |
| | Total Demand Duration [h] | 5258 | 3502 | 4851 | 3909 | 4007 | 4753 | 3343 | 2719 | 2056 | 6704 |
| | Ratio Total Duration to Core | 2.56 | 0.52 | 2.36 | 0.58 | 1.95 | 0.71 | 1.62 | 0.40 | 1.00 | 1.00 |